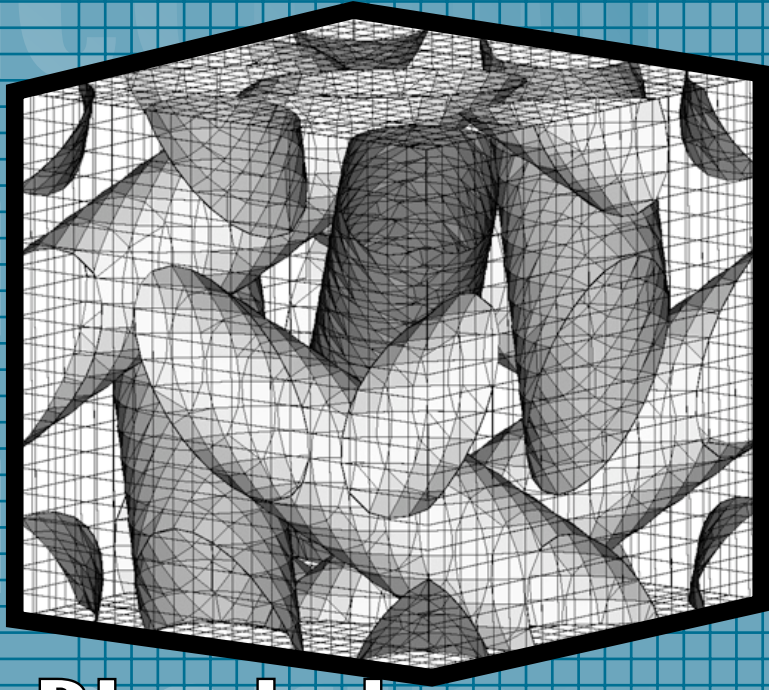


FY01 

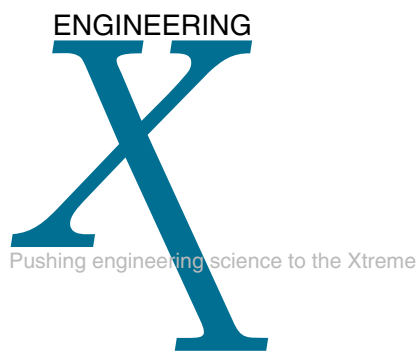
Engineering Technology Reports



Volume 1: Laboratory Directed Research and Development

September 2002

UCRL-53868-01



Acknowledgments

Scientific Editing

Camille Minichino

Graphic Design

Jeffrey B. Bonivert

Art Production/Layout

Debbie A. Marsh

Irene J. Chan

Lucy C. Dobson

Kathy J. McCullough

Document Approval and Report Services

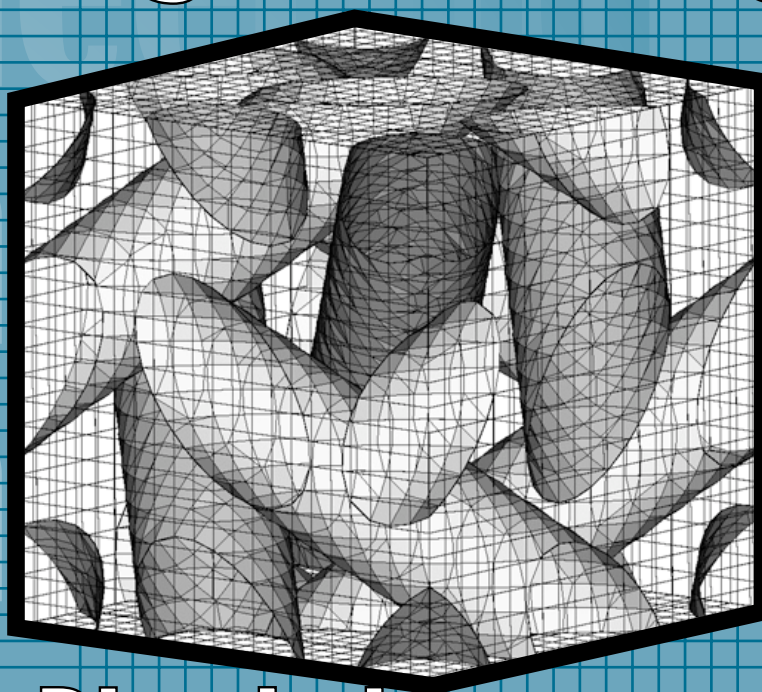
Cynthia Tinoco

Cover:

Stylized graphic of structured, extended finite-element refined mesh for unit cell analyses of fiber-reinforced composites.

FY01 

Engineering Technology Reports



Volume 1: Laboratory Directed Research and Development

September 2002

Introduction

<i>Glenn Mara, Associate Director for Engineering</i>	iii
---	-----

Center for Complex Distributed Systems

Cooperative Mobile Sensing Networks

<i>R. Roberts</i>	3
-------------------------	---

Developing Smart Seismic Arrays

<i>D. B. Harris, S. C. Larsen, D. B. McCallen, D. W. Rock, J. P. Lewis, D. H. McMahon, J. L. Levatin</i>	4
--	---

Hyperspectral Image-Based Broad Area Search (HIBAS)

<i>D. W. Paglieroni, D. E. Perkins, G. E. Ford (University of California, Davis)</i>	5
--	---

Ultra-Wideband Communications

<i>F. U. Dowl</i>	6
-------------------------	---

Center for Computational Engineering

Generalized Methods for Finite-Element Interfaces

<i>M. A. Puso</i>	9
-------------------------	---

Higher-Order Mixed Finite-Element Methods for Time-Domain Computational Electromagnetics

<i>N. J. Champagne, II, D. A. White, R. M. Sharpe</i>	10
---	----

Lattice Boltzmann Simulation of Microfluidic Devices

<i>D. S. Clague, E. K. Wheeler</i>	11
--	----

Modeling and Characterization of Recompressed Damaged Materials

<i>R. Becker</i>	12
------------------------	----

Numerical Technology for Large-Scale Computational Electromagnetics

<i>R. M. Sharpe, D. A. White, N. J. Champagne, II</i>	13
---	----

XFEM: Exploratory Research into the Extended Finite-Element Method

<i>K. D. Mish</i>	14
-------------------------	----

Center for Microtechnology

Acoustic Filtration, Fractionation, and Mixing in Microfluidic Systems

<i>K. Fisher, A. Wang, L. Tarte, C. Lee, W. Benett</i>	17
--	----

Disposable Polymerase Chain Reaction Device

<i>E. K. Wheeler, W. Benett, K. Ness, P. Stratton, J. Richards, T. Weisgraber, A. Papavasiliou</i>	18
--	----

Force-Feedback Instrument for Telerobotic Minimally Invasive Surgery <i>R. R. Miles, K. Seward, F. Tendick, W. Bennett, L. Bentley, P. Stephan</i>	19
Integrated Microfluidic Fuel Processor for Miniature Power Sources <i>J. D. Morse, A. F. Jankowski, R. T. Graff, J. P. Hayes</i>	20
Modeling Tools Development for the Analysis and Design of Photonic Integrated Circuits <i>T. C. Bond, J. K. Kellman, G. H. Khanaka, M. D. Pocha</i>	21
Palm Power: A MEMS-Based Fuel Cell/Integrated Microfluidic Fuel Processor <i>J. D. Morse, A. F. Jankowski, R. T. Graff, J. P. Hayes</i>	22
Reconfigurable Optical Code Division Multiple Access (O-CDMA) for Fiber Optical Networks <i>S. W. Bond, I. Y. Han, S. C. Wilks, E. M. Behymer, V. R. Sperry, S. J. Yoo (University of California, Davis)</i>	23

Center for Nondestructive Characterization

Dynamic Focusing of Acoustic Energy for Nondestructive Evaluation <i>J. V. Candy</i>	27
High-Accuracy Tomography of Mesoscale Targets <i>W. Nederbragt, S. Lane, D. Schneberk, T. Barbee, J. L. Klingmann</i>	28
New Simulation and Reconstruction Algorithms for Quantitative Tomography <i>M. B. Aufderheide, III, H. E. Martz, Jr., D. M. Goodman, A. Schach von Wittenau, C. M. Logan, J. A. Jackson, D. M. Slone, J. M. Hall</i>	29
Photothermal Imaging Microscopy <i>D. Chinn, R. Huber, C. Stolz, P.-K. Kuo (Wayne State University)</i>	30

Center for Precision Engineering

Predicting Precise Deformation of Non-Rigid Objects <i>K. L. Blaedel, D. W. Swift, A. A. Claudet</i>	33
--	----

Author Index

Author Index	37
---------------------------	----

Introduction

Glenn Mara, Associate Director for Engineering

Engineering has touched on every challenge, every accomplishment, and every endeavor of Lawrence Livermore National Laboratory during its fifty-year history.

In this time of transition to new leadership, Engineering continues to be central to the mission of the Laboratory, returning to the tradition and core values of E. O. Lawrence: science-based engineering—turning scientific concepts into reality.

This volume of Engineering Technical Reports summarizes progress on the projects funded for Laboratory Directed Research and Development (LDRD), supporting high-risk, potentially high-value R&D. LDRD projects serve as a proving ground for new research, enhancing the Laboratory's ability to address future DOE/NNSA missions, fostering creativity, and stimulating exploration at the forefront of engineering science and technology.

LDRD projects include:

- projects in the forefront of basic and applied science and engineering, for the primary purpose of significantly advanced laboratory capabilities;
- advanced studies of new hypotheses, experimental concepts, or innovative approaches to scientific and engineering problems;
- experiments and analyses directed toward "proof of principle," or early determination of the utility of new scientific and engineering ideas, technical concepts, or devices;
- preliminary technical analysis of experimental facilities or devices.

Five Centers focus and guide longer-term investments within Engineering. The Centers attract and retain top staff, develop and maintain critical core technologies, and enable programs. Through their LDRD projects, they help maintain the scientific and technical vitality of the Laboratory. The Centers and their leaders are as follows:

- Center for Complex Distributed Systems:
David B. McCallen
- Center for Computational Engineering:
Robert M. Sharpe
- Center for Microtechnology:
Raymond P. Mariella, Jr.
- Center for Nondestructive Characterization:
Harry E. Martz, Jr.
- Center for Precision Engineering:
Keith Carlisle

FY2001 Center Highlights

The **Center for Complex Distributed Systems** exploits emerging information technologies to develop unique communications related to data gathering, advanced signal processing, and new methodologies for assimilating measured data with computational models in data-constrained simulations of large systems. Effective combination of data and simulations leads to enhanced understanding and characterization of a breadth of complex systems ranging from large applied physics experiments to underground structures and missile defense systems. The Center's current research and development activities include: development of wideband communications for enabling robust and stealthy communications in a cluttered environment; autonomous airborne vehicle data collection from large, distributed sensor networks; advanced signal processing algorithms for wide area search with hyperspectral image data; simulation and imaging of underground facilities via matched field processing with massively-parallel seismic wave simulations and measured field data; and regional scale estimations of ground motions and infrastructure response in support of enhanced nuclear test readiness.

Currently the Center is supporting collaborations with seven faculty members from the University of California and the University of Nevada, and has co-sponsored research with the Nonproliferation Arms Control and International Security, Computations, Physics and Advanced Technologies, and Energy and Environmental Directorates at LLNL.

The **Center for Computational Engineering** orchestrates the research, development and deployment of software technologies to aid in many facets of LLNL's engineering mission. Computational engineering has become a ubiquitous component throughout the engineering discipline. Current activities range from tools to designing the next generation of mixed-signal chips (systems on a chip) to full scale analysis of key DOE and DoD systems.

Highlights of the Center's LDRD projects for FY2001 include generalized and higher-order mixed finite-element methods; lattice-Boltzmann simulation of microfluidic devices; modeling and characterization of recompressed damaged materials; and exploratory research into the extended finite-element method.

The mission of the **Center for Microtechnology** is to invent, develop, and apply microtechnologies for

LLNL programs in global security, global ecology, and bioscience. The Center is responsible for multidisciplinary integration of micro-technology. Its capabilities cover materials, devices, instruments, or systems that require microfabricated components, including micro-electromechanical systems (MEMS), electronics, photonics, microstructures, and microactuators. Center staff have achieved considerable national recognition for the successes demonstrated in Chem-Bio National Security Program instrumentation, supported by the DOE and the Defense Intelligence Agency.

Center highlights in FY2001 include advances in acoustic filtration, fractionation, and mixing in microfluidic systems; an integrated microfluidic fuel processor for miniature power sources; modeling tools development for the analysis and design of photonic ICs; and a reconfigurable optical code division multiple access device for fiber optical networks.

The **Center for Nondestructive Characterization** advances, develops and applies nondestructive characterization (NDC) measurement technology to significantly impact the manner in which LLNL inspects, and through this, designs and refurbishes systems and components. The Center plays a strategic and vital role in LDRD by researching and developing NDC technologies, such as acoustic, infrared, microwave, ultrasonic, visible, and x-ray imaging, to allow future incorporation of these new capabilities into LLNL and DOE programs. The near-term strategic mission objectives are to advance Engineering's core competencies and technologies in quantitative NDC and in fast nano-scale 3-D imaging.

FY2001 research contributions are in quantitative tomograph simulations and reconstruction algorithms;

photothermal microscopy: next-generation nanoscale imaging; and Wölter x-ray imaging optics for nanoscale digital microscopy and tomography.

The **Center for Precision Engineering** is dedicated to the advancement of high-accuracy engineering, metrology and manufacturing. The Center is responsible for developing technologies to manufacture components and assemblies at high precision and low cost; developing material removal, deposition, and measurement processes; and designing and constructing machines that embody these processes.

The scope of work includes precision-engineered systems supporting metrology over the full range of length scale, from atom-based nanotechnology and advanced lithographic technology to large-scale systems, including optical telescopes and high energy laser systems. A new focus is the manufacturing and characterization of "meso-scale devices" for LLNL's NIF. Millimeter-scale physics experiments will provide data about shock physics, equation of state, opacity, and other essential measurements of weapons physics.

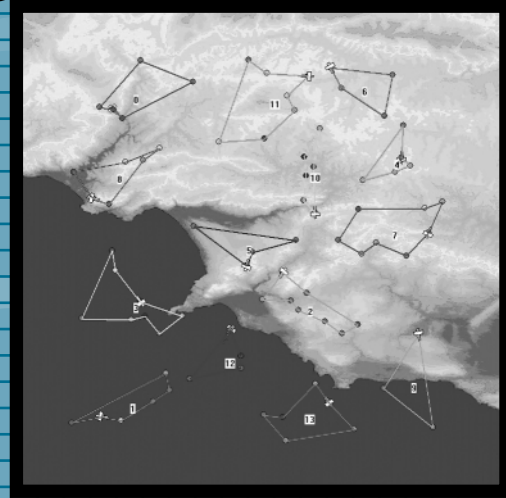
FY2001 highlights include a project to predict precise deformation of non-rigid objects.

Science-Based Engineering

Our five Centers develop the key technologies that make Laboratory programs successful. They provide the mechanism by which Engineering can help programs attract funding, while pioneering the technologies that will sustain long-term investment.

Our Centers, with staff who are full partners in Laboratory programs, integrate the best of mechanical and electronics engineering, creating a synergy that helps turn the impossible into the doable.

Center for Complex Distributed Systems



Technology

Cooperative Mobile Sensing Networks

R. Roberts

The objective of our LDRD project is to investigate the use of Unmanned Air Vehicles (UAVs) as an adaptive communications backbone for ground-based sensor networks. We are developing design guidelines for such a network, and are devising a theory of network operation. To support these goals, we are developing hardware and software, and conducting field tests of critical technologies.

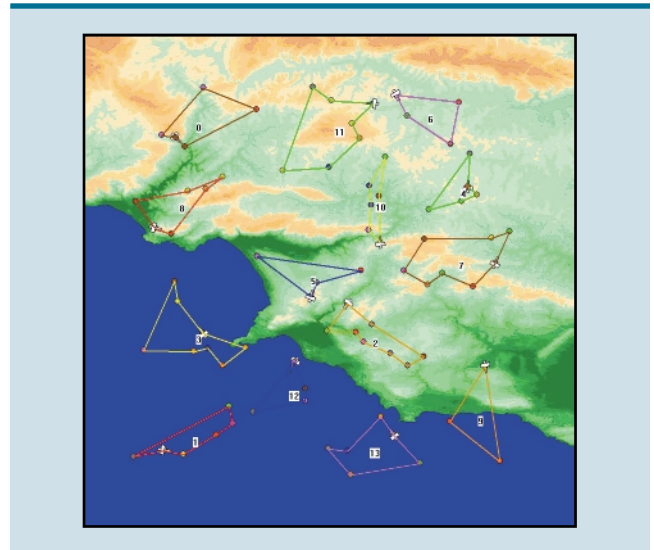
During FY01, we made many advances toward our objectives. With regard to UAV and network automation, we continued development of our path planning algorithm that began in FY00. Numerous improvements to the basic algorithm include: 1) addition of weights to sensor nodes; 2) addition of terrain constraint in path planning; and 3) improvements that decreased computational complexity. We wrote a paper, "An Adaptive Path Planning Algorithm for Cooperating Unmanned Air Vehicles," and presented it at the IEEE International Conference on Robotics and Automation, Seoul, Korea, May 2001.

Finally, we have begun to develop a mathematical model of network connectivity. The model is based on the paths of the UAVs, and is amenable to state estimation techniques, which will be developed in the third year of the project.

Our simulation code, (STOMP, for Simulation, Tactical Operations and Mission Planning), begun in FY00, has evolved beyond its original design. STOMP maintains and displays the states of objects (e.g., sensors and UAVs) over a digital terrain elevation data (DTED) background (see figure). An event queue associated with each object processes events by either time stamp or priority, thereby allowing external events (state updates from a real UAV) to be processed with simulated events (state updates from a simulated UAV). A message handler associated with each object determines the appropriate action for each type of event. Furthermore, the code is designed with an object hierarchy that allows the easy addition of new features and algorithms.

In the area of network communications, we have investigated various technologies required to implement architecture. As a result of the investigation, we have identified and obtained software technology that provides a store-and-forward service. This software has been tested on a desktop network, and is awaiting flight tests. We have built and tested several communications modules, using design ideas from our FY00 research and a TechBase project. These communication modules have been installed in our UAVs, and are awaiting flight tests.

During FY01, we established a collaboration with the University of California at Davis. The objective of this collaboration is to investigate algorithms that allow a UAV to adaptively search for point targets (i.e., a ground sensor uplinking data) given the general location of the target; to loiter in the vicinity of the target to collect data; and to move on to the next target after data collection is complete.



STOMP console, illustrating a network of 14 UAVs servicing 79 sensors.

Developing Smart Seismic Arrays

D. B. Harris, S. C. Larsen, D. B. McCallen, D. W. Rock, J. P. Lewis, D. H. McMahon, J. L. Levatin

Several important military and surveillance applications require imaging structures or tracking vehicles through uncertain and heterogeneous geologic media. Passive and active seismic methods are among the most promising techniques for solving these problems. However, past attempts at imaging and tracking applications often have performed poorly because insufficient attention was paid to characterizing the propagation medium or adapting algorithms to handle large uncertainties in medium parameters. This project examines two problems: tracking vehicles with seismic arrays on battlefield-scale problems, and delineating underground structures with signals observed by surface sensor arrays.

Both passive and active methods can be used to image underground structures. Passive methods use signals originating in the structure; active methods use surface sources (e.g., explosions) to generate signals that reflect from the structure.

The tracking problem is simpler, 2-D, and was our mid-year FY01 starting point. The structure imaging problem is inherently 3-D, correspondingly more complex, and the subject of FY02 work.

We take both empirical and model-based approaches to solving these problems. Small-scale field trials provide data to test means for characterizing geologic and representative media, and to test robust tracking and imaging algorithms. Computer models generate synthetic data for more realistic, larger-scale problems. The models are intended to economically answer "what if" questions such as "what is the best configuration and number of sensors for detecting or mapping an underground structure?"

The models are being built on E3D, an established LLNL 3-D full-physics elastic wave propagation code. We plan end-to-end validation of these models by simulating data from field trials.

We carried out a vehicle tracking experiment, depicted in the figure, at the Nevada Test Site (NTS). Two arrays were deployed, one with 12 and the other with 13 research-grade seismic (GS-13) sensors. Our collaborator, the Nevada Army National Guard, supplied two M1A1 tanks. These were driven singly and in pairs along a set of test tracks to the northwest of the arrays.

The results of processing data to estimate vehicle position are shown in the figure. It depicts two superimposed temporal snapshots of a detection statistic that

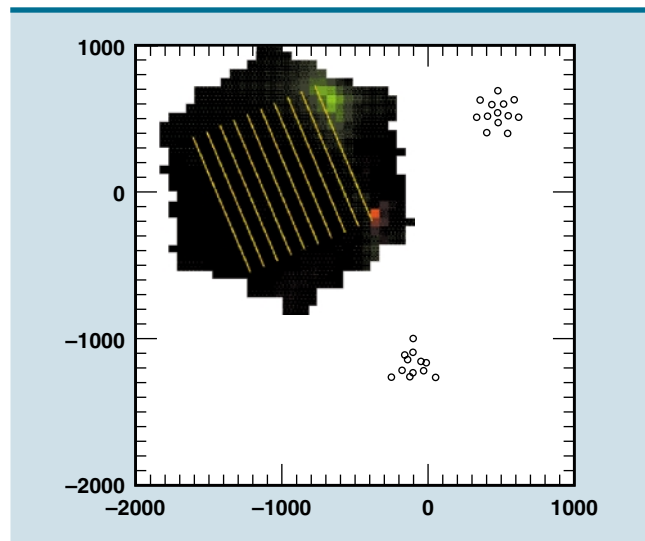
is large (bright) where the vehicle is most likely to be. The first snapshot (red) was taken as the vehicle began moving northward along the rightmost track indicated in the figure. The second snapshot (green) was taken minutes later as the vehicle approached the end of the track.

We developed and continue to develop basic software to support tracking and imaging applications. The software includes:

- a matched field processor for vehicle tracking,
- a framework for vehicle simulation, developed as a preprocessor for E3D to drive the code with equivalent seismic sources,
- initial work on a 3-D topography capability for E3D, essential for simulation in varied terrain.

In support of realistic vehicle simulation, we established ties with Professor Neil Perkins of the University of Michigan, who is developing an M1A1 simulator for the U.S. Army that can be coupled to our propagation model.

In preparation for next year's work, we scoped several venues at NTS and other locations for passive and active data collection above underground structures. Next year we will complete vehicle tracking simulation work, extend simulation to buried structure problems, extend our matched field processor to image underground structures, and collect data to test simulation and imaging algorithms.



Results of vehicle tracking experiment.

Hyperspectral Image-Based Broad Area Search (HIBAS)

D. W. Paglioni, D. E. Perkins, G. E. Ford (University of California, Davis)

From the standpoint of national security and non-proliferation, two of the most important tasks faced by image analysts are broad area search and site monitoring. In each case, the objective is to detect occurrences of targets of interest, typically solid targets of military significance or gaseous targets, such as active plume sources. In broad area search, large swaths of the countryside are imaged, usually once. In site monitoring, smaller areas of interest are imaged, potentially several times. To detect targets, one must compare target spatial and spectral signatures to signatures of pixel clusters extracted from overhead images. Hyperspectral imaging provides a tool for this purpose.

Hyperspectral images consist of hundreds of single band images stacked on top of one another, each corresponding to a different frequency in the infrared. As such, they provide a much greater context for both spatial and spectral signatures than conventional single band images, and are thus potentially far more useful for broad area search and site monitoring. Unfortunately, image analysts do not always have time to prepare reports on all of the conventional single band imagery presented to them, let alone hyperspectral imagery, which is far more voluminous.

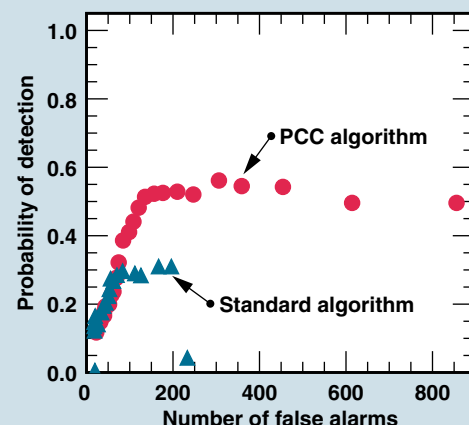
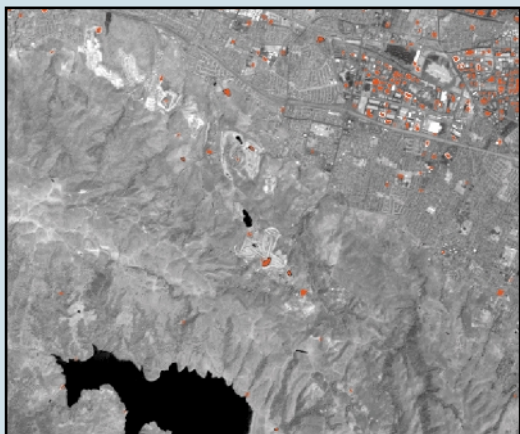
To address the analysis throughput problem without compromising target detection performance, it is useful to employ a model in which imagery from a broad area cueing sensor is used to task cued sensors to acquire suspected point targets. The cueing sensor is a hyperspectral imager that operates in push-broom mode, *i.e.*, it acquires imagery as the collection platform (*e.g.*,

aircraft) flies. This imagery is routed to an onboard processor which hosts algorithms that perform automatic target cueing (ATC) in real-time (*i.e.*, at image acquisition rates).

The ATC algorithms currently available are based on anomaly detectors that classify individual pixels as type "anomaly" or "background clutter." They routinely miss too many targets or produce too many false alarms. The goal of the HIBAS project is to develop, test, and evaluate two radically different ATC algorithms based on pixel clustering, as opposed to anomaly detection.

The first of these, Pixel Cluster Cueing (PCC), was developed at LLNL in FY01. The second, K-Means Re-Clustering, is under development at UCD, in conjunction with LLNL. The figure shows that PCC is able to efficiently detect more targets (red clusters on background image) at a given false alarm rate than the industry standard RX algorithm. The plots of detection probability vs. number of false alarms are generated by varying a decision threshold, and are based on a strict metric which undercounts hits and overcounts misses, but which is nonetheless useful for algorithmic comparison.

In FY02, the focus of HIBAS will be to complete the K-Means Re-Clustering algorithm, to augment PCC to optionally process individual spectral sub-bands, to improve spatial signature analysis, and to introduce spectral signature analysis, into the ATC process. Industry-standard algorithms will be compared against the HIBAS algorithms in a substantial study of ATC performance on hyperspectral imagery from a particular flight campaign used throughout the community.



Target cues for small buildings, and statistical performance of PCC vs. industry standard.

Ultra-Wideband Communications

F. U. Dowla

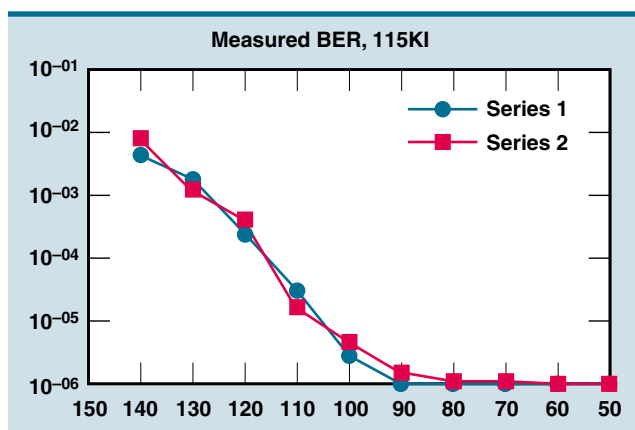
Several LLNL programs pursuing national security work require both low probability of detection and low probability of intercept in communication systems for clandestine urban and battlefield operations. The goal of the ultra-wideband (UWB) communications project is to develop advanced systems for covert wireless communications. These systems will fulfill important needs of the defense and intelligence communities of our nation.

Commercial communication systems that operate in fixed frequency bands are easily detectable and prone to jamming by the enemy. In many intelligence applications, it is often necessary to rapidly collect data, and transmit the data covertly and reliably. Robust communication links between the sensors collecting the data is a critical issue for demonstrating distributed sensor network performance in real-time.

In our first year of work in FY01, we have made significant progress towards a highly covert UWB radio. Several UWB radios have been designed, implemented, and tested with data and voice communication. We have completed the system architecture options and the modeling and propagation simulation studies with experimental validation.

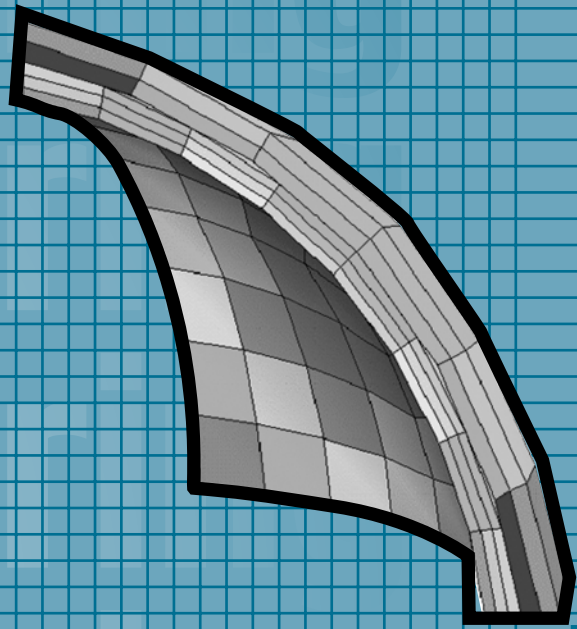
During the course of this year's work we found it challenging to meet the requirements for data capacity

(bits per second) and range, at the same time. Our goal for FY01 was a UWB radio at 200 kbps with a range of 100 m. Our design exceeded the data capacity by more than an order of magnitude (>2 Mbps). We have transmitted to about 10 m at that high data rate. However, as shown in the figure, we have just completed a test of our latest design with a radio that was able to transmit up to a range of 110 m at 115 kbps with a bit error rate of better than 0.0001. For this test, the data capacity was limited by the laptop computer test equipment.



Test results for data capacity and range.

Center for Computational Engineering



Technology

Generalized Methods for Finite-Element Interfaces

M. A. Puso

With the increasing complexity of finite-element models, it has become essential to mesh individual parts of a finite-element model independently, such that nodes at part boundaries are not aligned (see figure). In our work, new accurate numerical methods have been researched and developed to solve the problem of connecting dissimilar meshes. With these new methods, it will no longer be imperative to produce conforming meshes.

The current finite-element methods for connecting (i.e., gluing, tying) dissimilar meshes together at the boundary often cause serious errors in a stress analysis. Aware of this fact, analysts work to avoid dissimilar meshes, but often to no avail. Furthermore, it has become the trend for different analysts or teams of analysts to work independently on different weapons subassembly meshes, which are ultimately combined into a single finite-element analysis. This type of design paradigm *always* requires the connection of dissimilar meshes and *demands* more robust and accurate methods for handling the interfacing of parts.

We have researched and developed new accurate numerical methods to solve the problem of connecting dissimilar meshes. This new technology can potentially save the programs vast amounts of time and money. For example, a large weapons model often takes a month to build and will see many revisions over a matter of years. Analysts estimate that a method for connecting dissimilar meshes may save up to 25% of their time in meshing.

In particular, small modifications to a large model often required reworking the entire model. Now, a new feature can be “attached” to a current model while leaving the remaining model unaffected.

Recent work in the area of domain decomposition produced the so-called “mortar method” for connecting 2-D flat interfaces. In FY01, we extended the mortar method to connect arbitrary 3-D curved meshes so that optimal convergence is achieved. In this way, mesh refinement of the dissimilar mesh will have the same asymptotic rate of convergence as the conforming mesh. Consequently, the use of dissimilar meshing will not compromise the quality of a mesh. Our FY01 work focused on the following issues:

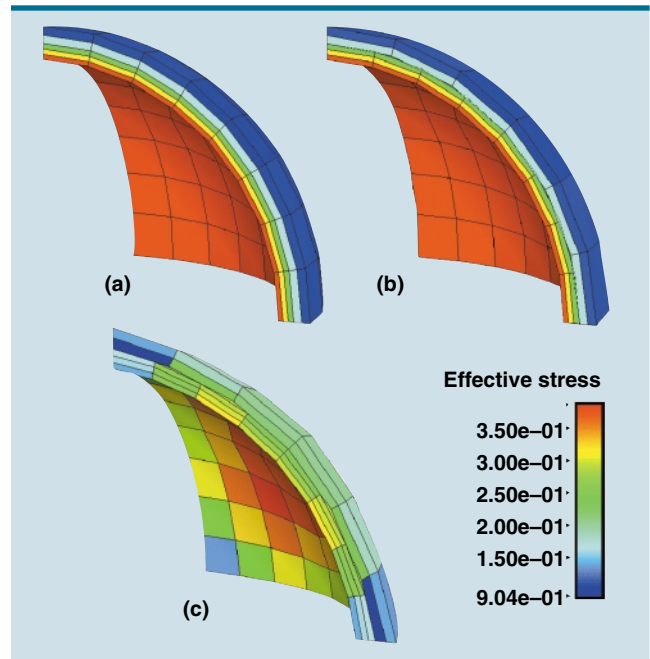
1. How are projections from adjacent dissimilar meshes to be made?
2. What type of integration will be used for the numerical evaluation of the variational projection operators?

3. What Lagrange multiplier traction interpolation fields are to be used?
4. How will conservation of linear and angular momentum be preserved?

So far we have identified several approaches and have implemented them in NIKE3D. One important discovery was the need for using a Lagrange multiplier traction field that was one order lower than the displacement field. It has been demonstrated that these lower-order fields are necessary for retaining optimal convergence when the dissimilar mesh boundary is curved.

The new methods appear to work remarkably well. For example, the figure (a-c) shows the stresses from an analysis of an internally pressurized sphere. The stresses in the conforming mesh (a) differ by only 0.29% when compared to the dissimilar mesh (b), where the new mortar method was used. Stresses computed using the old collocation method shown in the figure (c) differ by 58%.

FY02 work will involve the extensions to higher-order element meshes and contact surfaces.



Stress contour of an internally pressurized sphere. (a) Conforming mesh. (b) Dissimilar mesh using new mortar method. (c) Dissimilar mesh using old collocation method.

Higher-Order Mixed Finite-Element Methods for Time-Domain Computational Electromagnetics

N. J. Champagne, II, D. A. White, R. M. Sharpe

Computational electromagnetics (CEM) is the most cost-effective approach for electromagnetic design and analysis, and often the only alternative due to safety, legal, and other issues. LLNL does not have a robust, unstructured grid, time-domain CEM code. While some research on mixed finite-element methods (MFEM) for time-domain CEM has been performed in academia, there are no commercial or government codes that use this methodology. Hence, this is a unique opportunity for LLNL not only to resolve an internal problem, but also to regain prominence in the CEM community.

CEM is a core competency of the Engineering Directorate. This project is aligned with the mission of the Center for Computational Engineering, which is to develop large, parallel, complex computational modeling and simulation tools for Engineering. There are many applications that are inherently temporal in nature (e.g., very rapid rise times), and a robust time-domain capability that scales up to the required complexity is essential to meet the charter of the Engineering Directorate. In addition, multi-physics solutions are becoming more important, and this activity is essential to facilitate close coupling with the analysis of other disciplines.

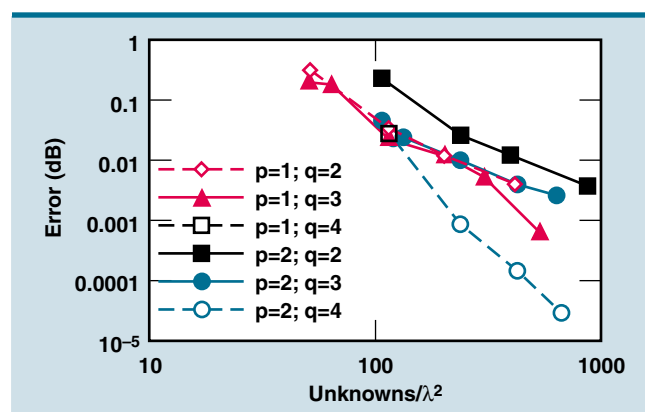
Our approach is to research and apply modern MFEM for the solution of partial differential equations on 3-D unstructured grids. In MFEM, different basis functions are used for different physical quantities. This has several benefits, such as proper modeling of electromagnetic boundary conditions across material discontinuities, numerical stability, and strict conservation. In addition, the use of higher-order approximations, which is problematic for finite-difference and finite-volume schemes, will enable the efficient modeling of electrically large problems.

In FY01, a major decision on implementing higher-order MFEM was to determine if an existing code framework would allow a tractable extension to higher-order elements and basis functions. It was determined that it would be more efficient to use a validated frequency-domain electromagnetics code (EIGER),

instead of creating a comparable time-domain framework to test the new higher-order structures. The types of higher-order bases added to date include the scalar bases, curl-conforming vector bases (except for segments), and divergence-conforming vector bases of general order for the elements listed previously.

An example of the benefits of higher-order modeling is shown in the figure, which consists of a plot of the RMS error of the radar cross-section of a perfectly conducting sphere as the unknown count is increased. The error is best reduced by using a fourth-order element with a second-order basis function.

In FY02 we will carry out both mathematical analysis and computational experiments to quantify the accuracy and robustness of the method. Specifically, we will verify the higher-order rates of convergence for time-domain computations. In addition, higher-order time integration schemes, both explicit and implicit, will be investigated. Fast methods will be required for solving linear systems at every time step. The solver libraries from the LDRD project, "Numerical Technology for Large-Scale Computational Electromagnetics" will be applied to the linear systems. Also, a framework will be designed to facilitate future changes or additions to the time-domain or solver methods. Naturally, many iterative refinements to the software will be performed during the second year.



The RMS error of the radar cross-section of a perfectly conducting sphere as the number of unknowns increases.

Lattice Boltzmann Simulation of Microfluidic Devices

D. S. Clague, E. K. Wheeler

In microfluidic devices, fluids, beads, and other biological matter are transported through networks of micrometer-sized channels for sample preparation, separations, and assays. Understanding the transport behavior of target species in these devices is of paramount importance. The lattice Boltzmann (LB) simulation effort has grown out of a need for computational tools to assist the designers of microfluidic and of biological microfabrication and microelectromechanical systems (bio-MEMS) devices to predict and understand the behavior of beads and macromolecules in microflows.

The LB simulation capability, which is a significant advancement over current methods, takes into account the multiple, competing physical phenomena that take place in actual devices—for example particle dynamics, external fields, and near-field particle–particle, and particle–wall interactions.

Our goal has been to develop a simulation capability to explore the incremental, additive effects of these interactive forces, to 1) facilitate understanding, and 2) explore new means of particle manipulations. In particular, work has focused on characterizing particulate behavior in dielectrophoretic separators.

Particle mobilities are influenced not only by the colloidal interactions, but also by non-Newtonian fluid effects and particle geometries. Therefore, we enhanced the LB capability to handle bead-and-spring representation of species, and power-law fluids (many fluids containing biological species—biofluids—exhibit nonuniformity in viscosity caused by variations in fluid velocity, also known as shear-thinning behavior). With these enhancements, the LB capability will be applicable to a broader class of biofluidic systems.

As described above, the viscosities of biological fluids tend to depend on the local shear rate. As a result, particle mobilities can be significantly affected and exhibit nonintuitive behavior. In FY01 we modified the collision operator in the LB formulation to take into account local changes in the shear rate. Comparison of results from the new, enhanced LB capability and theory are shown in the figure.

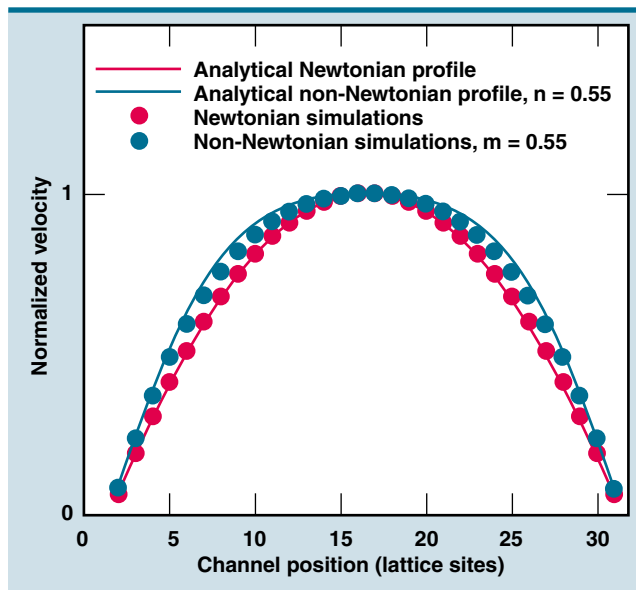
We compared the shear thinning and thickening behavior as predicted by the enhanced LB capability with power-law fluid theory for flow between parallel plates. As shown in the figure, the simulated results are

in good agreement with theory. Furthermore, as discussed above, we enhanced the LB simulation capability to account for more complex particle features.

Many species of interest (e.g., DNA strands) are best represented as long chains; hence, one aim of this year's effort was to develop a bead-and-spring representation of macromolecules.

To accomplish this, we successfully incorporated the Finite-Extension-Nonlinear-Elastic-Dumbbell (FENE-Dumbbell) model into the LB capability. The model provides both a building block for representing long-chain macromolecules in the LB simulation capability and the “spring” that bridges the beads—and which also causes the bulk fluid to have non-Newtonian behavior.

The enhancements that we developed over the past year have expanded the applicability of the LB capability. Specifically, with the bead-and-spring representation of macromolecules, researchers will be able to study the influence of the chain dynamics of target species—such as a biological agent—on transport properties, and conformational issues relevant to detection. Furthermore, the ability to capture the shear-thinning behavior, without any increase in computational time, positions this capability for application to many new problems involving biofluids.



Lattice Boltzmann prediction of power-law fluid behavior compared with theory.

Modeling and Characterization of Recompressed Damaged Materials

R. Becker

Ductile metals subjected to shock loading can develop internal damage through nucleation, growth, and coalescence of voids. The extent of damage can range from a well-defined spall plane induced by light shocks to more widespread damage caused by strong shocks. Damaged materials are often part of a dynamic system, and significant additional deformation can occur in extensively damaged materials. To represent material behavior in simulation codes accurately, it is necessary to model the recompression behavior in addition to the damage processes. Currently, there are no experimentally-based models of recompression behavior available for use in numerical simulations.

The goal of this project is to perform recompression experiments on samples with controlled and well-characterized damage; develop a model capturing the recompression behavior and residual strength; and implement the model in an ASCII code. The recompression model, together with physically motivated failure models, will provide a more accurate representation of material behavior needed for simulations of explosively loaded materials and stockpile stewardship simulations.

The experimental work is being done in three sequential stages: 1) creating controlled initial damage in the form of a spall plane using a light gas gun; 2) measuring the material response during compression of samples excised from the soft-recovered specimens; 3) assessing the residual strength of the recompressed material.

In FY01, a gas gun with a newly-developed soft recovery capability was used to create spall damage within copper specimens. The level of damage ranges from insignificant to incipient fracture along a spall plane. The targets were sectioned and the damage level recorded using optical metallography. The montages of micrographs have been digitized and analyzed to characterize the magnitude and extent of the damage.

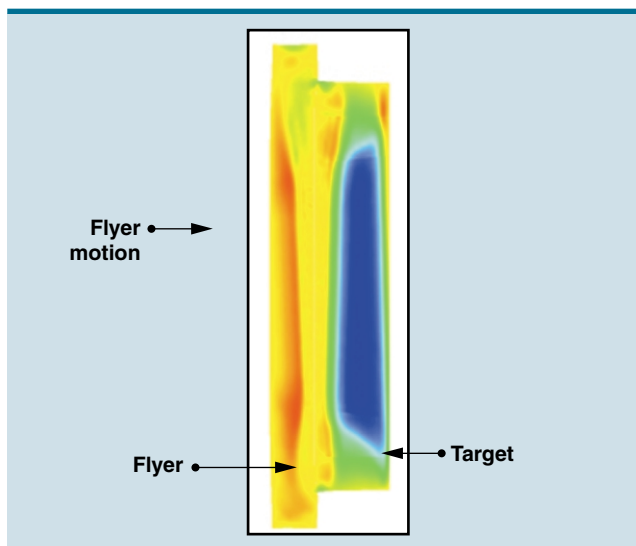
From each of the gas gun targets, four cylindrical specimens were extracted for subsequent experiments. Having multiple samples with the same loading history and damage will facilitate determination of effects of recompression rate as a function of damage level.

Modeling work was performed in support of the gas gun and recompression experiments. The gas gun

experiments were simulated using a damage evolution model to determine the extent of the uniformly damaged region. This information was used in specifying the size and location of the recompression specimens that were cut from the gas gun targets. Additional 3-D simulations were performed to examine effects of slight flyer misalignment on porosity distribution and the free surface velocity diagnostic (see figure).

Simulations of the split-Hopkinson bar recompression tests have also been performed to gain insight into the loading signals. Quantitative analysis of dynamic recompression tests is new, and modeling will be used as an aid in data interpretation.

Plans for FY02 are to complete the recompression tests and perform modified tensile experiments on the recompressed samples to assess the residual strength. Data from the recompression tests will be used either to modify an existing damage evolution model or to develop a phenomenological representation of the recompression behavior. The model will then be attached to an existing damage evolution model in an ASCII code for evaluation. Since this is a first-cut model based on limited data, it is only a first step toward developing an accurate and robust simulation capability for recompressed damaged materials.



Simulation of gas gun experiment used to determine effects of a 0.001-radian flyer misalignment on spall damage. Shown are contours of axial stress.

Numerical Technology for Large-Scale Computational Electromagnetics

R. M. Sharpe, D. A. White, N. J. Champagne, II

The key bottleneck of implicit computational electromagnetics (CEM) tools for large, complex geometries is the solution of the resulting linear system of equations. The goal of this project is to research and develop numerical technology that alleviates this bottleneck for large-scale CEM by greatly reducing the time required to solve the associated hybrid linear systems of equations.

The mathematical operators and numerical formulations used in this arena of CEM yield linear equations that are complex-valued, unstructured, and indefinite. Also, simultaneously applying multiple mathematical modeling formulations to different portions of a complex problem (hybrid formulations) results in a mixed structure linear system, further increasing the computational difficulty.

Typically, these hybrid linear systems are solved using a direct solution method, which was acceptable for Cray-class machines but does not scale adequately for ASCI-class machines. Additionally, LLNL's existing linear solvers are not well-suited for the linear systems that are created by hybrid implicit CEM codes.

During FY00, our activities focused first on establishing a test suite of sample matrices to evaluate the solver research. Next, we chose the ISIS++ solver framework (developed at Sandia National Laboratories, Livermore) as a basis for our research. We extended this package to treat complex-valued, hybrid linear systems. In addition to the native iterative methods in the package, we added several direct solvers to address the hybrid linear system.

Our FY01 activities began with an implementation of a Shur-complement approach for solving block-structured hybrid linear systems, which greatly improves the speed

of solution. In addition, we identified and addressed the key research issues associated with preconditioners. In some cases, we extended existing preconditioners to apply to the operators in CEM; in others, we developed more physics-based operators.

We identified the need for a research effort on both matrix-based and operator-based preconditioners. The matrix-based methods can be applied to any linear system of equations after the matrix has been assembled. We began work on sparse approximate inverse preconditioners and on incomplete lower/upper preconditioners (ILUs). This work will continue in FY02, with a new employee whose doctoral research was in parallel ILU methods.

We began a portion of the work on direct operator-based methods with R. J. Adams of the University of Kentucky. The methods here are to recast integral equations of the first kind into integral equations of the second kind, which we expect to greatly improve the basic conditioning of the linear system. An overall improvement of the system conditioning has been shown to significantly reduce the solution time. We made some progress in this direction, and further work on it is being actively pursued.

The next task was to begin research into so-called fast multipole solution methods (FMM). These methods have been shown to reduce the operation count from N^2 to $N \log(N)$ for linear systems to which they apply.

In FY02 we will focus initially on completing the additional matrix-based preconditioners and then on completing the operator-based work for important operators used in CEM. All of this work will be incorporated into our existing solver framework for delivery to LLNL researchers and to the CEM community at large.

XFEM: Exploratory Research into the Extended Finite-Element Method

K. D. Mish

The finite-element method has become the standard tool of computational mechanics in the national laboratory community, and it accounts for the vast majority of computational analyses performed in support of LLNL's mission. General-purpose finite-element LLNL physics codes such as DYNA3D and ALE3D represent the pinnacle of simulation-based practice in mechanical engineering. Unfortunately, conventional unstructured finite-element applications are optimized for the design of idealized mechanical systems, whereas LLNL's Stockpile Stewardship mission (for example) is more concerned with the analysis of as-built systems. With sufficient effort, efficient mechanical analysis of such systems can be achieved with tools optimized for general mechanical design.

The discrepancies between idealized and as-built mechanical configurations may be considerable, and may in fact render analyses based on the former woefully inadequate. There is a need to extend the domain of applicability of finite-element techniques to as-built mechanical simulations such as those found in various LLNL programs. Further, given the volume of such simulations being conducted, there is a need to automate the analyses to the greatest extent possible.

Extended finite-element (XFEM) techniques provide a means for addressing the "as-built vs. idealized" issue, because this family of improvements to conventional finite-element modeling permits a broader range of mechanics simulations of the actual configuration of the mechanical system. In addition, XFEM remedies some of the most onerous limitations of finite-element modeling relevant to LLNL's needs (e.g., localization and singular response near cracks and imperfections).

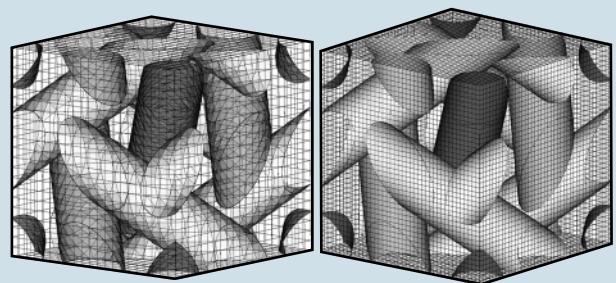
This project will substantially extend LLNL's core competence in computational science and engineering, and its capabilities in manufacturing and nuclear technologies.

In FY01, we began the design of a scalable high-performance framework for XFEM simulations. Although XFEM closely resembles conventional finite-element codes in many respects, there are also substantial differences that make it difficult to reuse code modules from existing finite-element tools. In addition, many of the programmatic drivers for XFEM at LLNL are oriented to manufacturing operations, which involve

long-duration physics. Scalable nonlinear implicit XFEM analyses, which can computationally span such long time intervals, are therefore of primary importance for manufacturing operations.

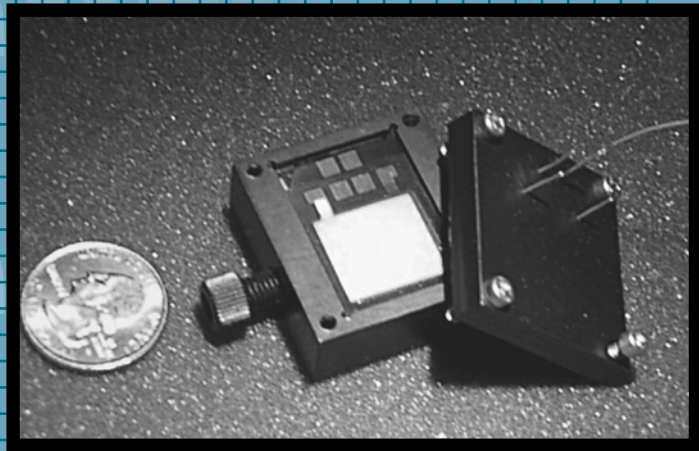
We began preliminary work on demonstrating the range of science and engineering problems that are amenable to solution with XFEM modeling techniques. One important case study, recently developed by our collaborators at Northwestern University, concerns the multiscale mechanical response of composite materials. This problem is attacked by decomposing a structurally anisotropic composite material into unit cells, which are the smallest components capable of representing the composition of the macroscopic material. Mechanical analysis of these unit cells, combined with consistent scale-bridging response-superposition techniques, now permits materials scientists to predict the response of engineered materials (such as composites or functionally graded materials) by standard mechanical simulation methods.

The figure shows how structured XFEM techniques can be used to capture the unit cell response of a fiber-reinforced composite (with fibers shown in light and dark gray). The fibers are embedded in a material matrix, which is not shown. Results obtained with the structured XFEM meshes shown agree in detail with those obtained in simulations performed using conventional unstructured finite-element techniques, but the XFEM meshes required an order of magnitude less effort to prepare, reducing weeks of preparation to days, and providing the results largely without human intervention. This demonstrates the fundamental goal of this project, that of analysis automation.



Structured, extended finite-element meshes for unit cell analyses of fiber-reinforced composites: left, coarse mesh; right, refined mesh.

Center for Microtechnology



Technology

Acoustic Filtration, Fractionation, and Mixing in Microfluidic Systems

K. Fisher, A. Wang, L. Tarte, C. Lee, W. Benett

This project is concerned with the research and development of a technique to manipulate small particles using acoustic energy coupled into a fluid-filled plastic or glass sample chamber. The resulting miniaturized systems combine high functionality with an inexpensive, disposable sample chamber.

A robust method for sample pretreatment that combines filtration, fractionation, and mixing of particles is an integral first step in the development of miniaturized microfluidic biological analysis systems. Typically, the cost of a part increases with its functionality, yet the danger of sample-to-sample contamination makes inexpensive, disposable parts attractive.

Our acoustic-based system results from a technique to manipulate small particles using acoustic energy coupled into a fluid-filled plastic or glass sample chamber. The system allows the performance of the basic fluidic functions necessary in an analysis system. The impact of this project is considerable for the microfluidic module (MFM), which is in direct support of the counter-bioterrorism project of NAI. In addition, emerging MEMS-based companies, such as Affymetrix, Caliper, and ACLARA, are targeting these types of miniaturized microfluidic systems for commercialization.

During FY01 we extended our understanding of the complex behavior of the acoustically-driven standing wave chambers by developing accurate 3-D multi-physics finite-element models using ABAQUS. With this sophisticated computational model, the electroacoustic response of the PZT transducers (acoustic sources) and the fluid-structure response of the chamber are analyzed simultaneously. From this numerical modeling, several significant improvements were made in the mixing and particle trapping (filtering) performance of the actual devices.

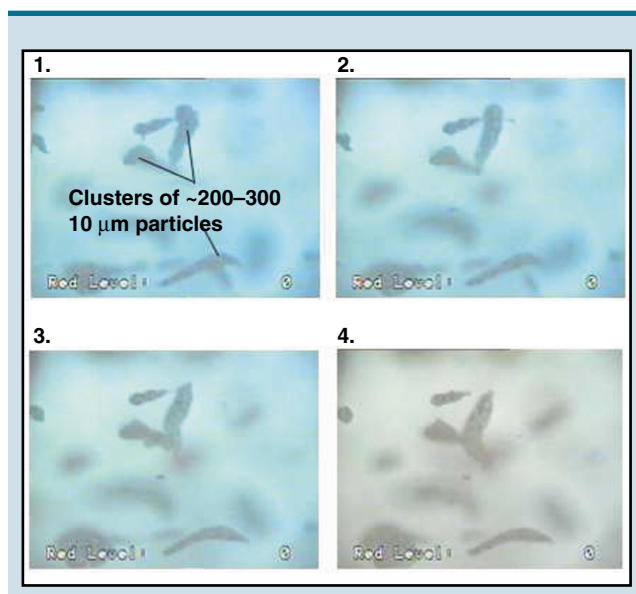
Also, because the new chambers have been acoustically optimized, they can be operated at lower drive voltages (5 to 15 Vpp, or approximately one third of the levels of the FY00 designs) with the same fluidic performance. The performance of these new devices is strongly dependent on the geometrical shape and construction tolerances.

A new glass chamber fabrication process was developed to construct the new borosilicate sample chamber prototypes. The resulting chambers have the planar

geometrical tolerances required to facilitate robust and stable standing wave patterns

The experimental efforts in FY01 were directed toward filtering and fractionation of a flowing sample volume. A typical process, "particle rinsing," is shown in the figure. A mixture of 10- μ m poly-beads and a reagent (DI water and blue dye) flows through the sample chamber. The particles are trapped and begin to collect at specific nodal positions in the acoustic field. When a sufficient number of particles have been trapped, a neutralizer (simulated here as DI water) is sent into the sample chamber, rinsing out the blue dye. Procedures such as this are commonly used to reduce background noise in a flow cytometer.

During this final year, we expanded the scope of the project to include applications where particles and or pathogens can be trapped and extracted from large volumes of water such as those routinely found in municipal water treatment systems. In addition, we are in the initial stages of developing a partnership with a company that has shown interest in our ability to induce acoustic mixing in microchambers. Finally, we also have a provisional patent (IL-10924) for the current prototypes.



Images taken at 10-s intervals show stationary particle clusters while the blue fluid is replaced with clear fluid. Volumetric flow is 0.15 ml/min.

Disposable Polymerase Chain Reaction Device

E. K. Wheeler, W. Benett, K. Ness, P. Stratton, J. Richards, T. Weisgraber, A. Papavasiliou

The September 11, 2001 attack on the United States raised anti-terrorist vigilance to new heights. While this attack was orchestrated with hijacked planes, the next threat could be nuclear, chemical, or biological. Many countries that may support terrorist activities are likely to have biological weapons capabilities. It is also possible that biological weapons are available on the black market. The U.S. needs to plan and equip for a biological terrorist attack. Planning for such an event requires that detection devices be robust in the field, easy to use, and relatively inexpensive. We are building a compact, disposable Polymerase Chain Reaction (PCR) unit. The end device from this project will allow first responders to the scene of a biological assault to quickly identify the nature and extent of that attack.

The role of PCR assays is becoming increasingly important in the quest to identify biological organisms. PCR allows one to amplify a target segment of DNA. First responders to a biological attack will need to identify the specific organism used in the release to initiate the appropriate course of action. Unfortunately, the types of sophisticated tools needed to assess a potential biological release are unaffordable to many first responding agencies and require highly trained individuals.

Building on LLNL's expertise in designing portable PCR units, this project seeks to develop even lower-cost, disposable PCR units to be used by first responders, military, or intelligence personnel.

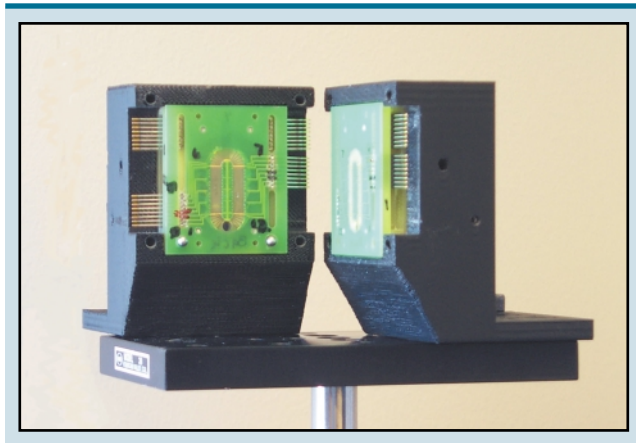
In addition to chemical and biological warfare applications, forensic organizations or environmental specialists looking for the source of contamination in food, or water remediation, will also benefit from this device.

FY01 resulted in prototypes of the novel thermal cycling chambers and design iterations from modeling. We have focused on designing and fabricating the thermal cyclers for PCR amplification. A new design for the thermal chamber uses fixed, non-fluctuating hotter and cooler temperature regions through which the sample fluid flows, driven by thermal convective forces.

The convective thermal cycler with zone heating is shown in the figure. As the fluid in the hot section heats to 95 °C, it is expected to circulate due to thermal convection to the cooler outer section. The advantage of this approach is that there is potentially a large energy savings, which increases the probability that small batteries will suffice as the power source for the system.

The first iteration of the convectively-driven cycler has been fabricated. Initial particle imaging has shown that natural convective forces are strong enough to drive the fluid around the chamber at reasonable speeds. Since the convective PCR thermal cycler is higher risk and has never been used to drive PCR, we have performed modeling to verify sufficient driving forces can be generated and to permit the selection of optimal materials and geometric parameters before fabrication. A patent application for the naturally-driven convective PCR thermal cycler has been submitted (ROI: IL10582).

Sample preparation and minimizing the power consumption of the thermal chamber will be addressed in FY02. Although the thermal cycler is the heart of the PCR amplification, sample integration and detection are crucial to our end deliverable of an integrated, easy-to-use, low-power, robust, and disposable PCR device.



Convectively-driven PCR thermal cycler.

Force-Feedback Instrument for Telerobotic Minimally Invasive Surgery

R. R. Miles, K. Seward, F. Tendick, W. Benett, L. Bentley, P. Stephan

The number of minimally invasive (MI) surgical procedures has risen steadily since the introduction of the concept in the late 1970s. In most MI procedures, the surgeon inserts rigid instruments through small incisions and manipulates them directly. Telerobotic, or master-slave robotic systems, have been introduced in the last few years to carry out MI procedures (such as those in the abdominal cavity) that require greater control and dexterity than humans can provide. The goal of this project is to improve the state of the art of MI telerobotic tools.

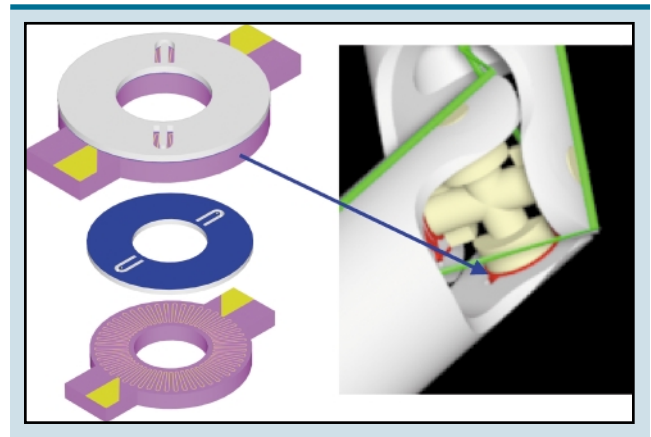
Two drawbacks limit the application of telerobotic systems to demanding procedures such as fetal surgery, beating-heart surgery, and tumor removal. First, the mechanical joints used in such systems are larger than is desirable. Second, control of the manipulators is not as precise as necessary because the positional and force-feedback sensors and the actuating motors are placed at the proximal end of the device, near the surgeon, rather than at the distal end, where the end-effectors are located. Control errors result from mechanical compliance (the deformation of the system under load) between the sensors and the manipulator.

Our goal is to improve the state of the art of MI telerobotic tools in several respects. First, we plan to improve dexterity by designing a manipulator with a wrist joint capable of a full three degrees of rotational freedom, to mimic that of the human wrist. We plan to reduce the overall size of the manipulator to enable surgery in more confined areas and to reduce patient trauma enough that local rather than general anesthesia can be used. Second, we plan to design microscale sensors to be inserted at the manipulator to increase the accuracy of the system's position and force feedback, and to develop a haptic feedback loop to give the surgeon a better "feel" of the instrument's motion. Third, we plan to design a compact actuator to be inserted near the end-effector to improve fine-motor control.

This project supports nascent programmatic efforts in medical technologies and has several potential military applications, including the use of remotely controlled surgical tools in the battlefield and the remote inspection and repair of unmanned machinery.

In FY00, we completed the prototype design of a wrist joint that is capable of meeting the dexterity requirements for this application. We completed the design and are starting to fabricate the microscale position sensors. A rendering of the resistive-capacitive sensor to be inserted in the end-effector is shown in the figure.

We have taken some steps toward building the joint and sensors to verify the designs. F. Tendick, a member of the UCSF Department of Surgery, is leading the control effort for the project. Tendick's two students and a postdoctoral fellow worked on developing the nonlinear control algorithms required for a proposed compact push-pull actuator using shape-memory alloy as the "muscle." A test-bed was designed and built for testing these algorithms.



Resistive-capacitive embedded sensor.

Integrated Microfluidic Fuel Processor for Miniature Power Sources

J. D. Morse, A. F. Jankowski, R. T. Graff, J. P. Hayes

Miniature fuel cells have attracted significant interest in recent years as a viable alternative for powering portable electronics. While hydrogen is the ideal fuel, reformate fuels are a viable option for the miniature fuel-cell power sources being developed at LLNL. These miniature fuel cells represent a unique approach, using thin-film solid-oxide electrolytes that operate in the 350 to 600 °C range and are tolerant of CO-poisoning effects. An integrated, microfluidic fuel processor, capable of reforming hydrocarbon-based fuels having high specific-energy contents, would provide significantly longer-lasting power sources than are now available. This work leverages LLNL's expertise in microfluidic devices, microfabrication techniques, and materials science.

Potential applications for miniature fuel-cell power sources include their deployment in the autonomous sensor networks being developed to meet national security requirements, and as battery replacements for a range of consumer electronics products—including cell phones and handheld computers.

The objective of this project is to design, fabricate, and test a microfluidic fuel processor that converts an easy-to-store liquid fuel, such as methanol, to hydrogen, as the fuel flows from the reservoir through a glass microchannel that has been coated with catalytic material.

During FY01, we designed, fabricated, and initiated testing of prototype fuel processors. The primary design, illustrated in the figure (a), consists of a glass microchannel that is coated with a catalytic material and connected to the fuel reservoir by microfluidic interconnections. Resistive heaters positioned along the reaction zone allow the fuel mixture to be heated as fuel flows through the microchannel.

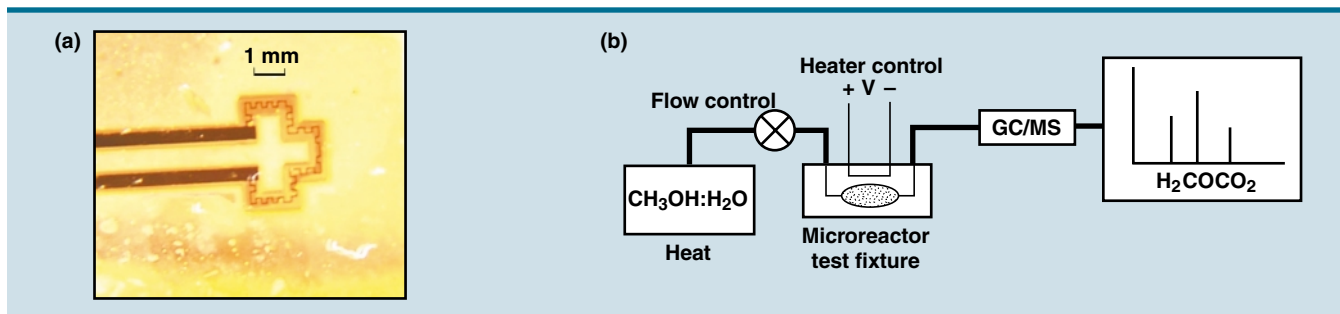
With water added to the methanol, the steam-reforming reactions are assisted by the catalyst at

temperatures in the 200 to 300 °C range, which is compatible with our solid-oxide fuel-cell operating temperature. Steam reforming reacts methanol and water, generating byproducts of hydrogen, carbon monoxide, and carbon dioxide.

With adequate surface area of the catalytic material and applied heat, the microfluidic reformer produces hydrogen-gas fuel with minimal power input required to sustain the microreaction. Thus, the design details of the microchannel fuel processor must specifically match the necessary volume, catalyst surface area, flow velocity, and thermal signature of the glass microchannel. The hydrogen and other byproducts are then delivered to the fuel-cell manifold by microfluidic interconnects. This system approach allows an integrated solution that addresses issues of fuel storage, processing, and delivery. The goals of this effort are reforming sufficient methanol to generate 500 mW of electrical power from a fuel cell.

The figure (b) shows the experimental apparatus to evaluate the performance of our fuel processor. Initial testing demonstrated conversion of the methanol–water fuel mixtures at very small flow rates, corresponding to the effective surface area of the catalyst support. Thus, for a Pt catalyst coated by evaporation into glass microchannel reactors having a total length of 4 cm, we observed that conversion to byproducts, including carbon dioxide, began at 240 °C. Further quantification of conversion efficiency will determine the optimal flow velocity of specific microchannel designs and catalyst materials.

In FY02, we will continue to explore the optimal catalytic material for incorporation within our microfluidic device. We will also further evaluate additional issues, such as the heat-transfer characteristics of the reformer itself, effective heat-exchange designs, and specific flow rates.



A new, microfluidic fuel processor, showing (a) the glass-microchannel reactor with its integrated resistive heater; and (b) the experimental apparatus (GC/MS is a gas-chromatography mass spectrometer).

Modeling Tools Development for the Analysis and Design of Photonic Integrated Circuits (ICs)

T. C. Bond, J. K. Kellman, G. H. Khanaka, M. D. Pocha

We are witnessing a “photronics revolution” in which photonic ICs are the major players. Highly compact, low-latency (sub-ps), wide-bandwidth (THz), ultra-fast (100 Gb/s) digital-logic and secure-information systems are potentially feasible. However, because industry focuses on high-bandwidth, fiber-optic telecommunications, commercial software is limited to meeting a restricted suite of problems. Thus, as devices increase in complexity, new components cannot be modeled accurately using existing numerical methods. Our goal is to create state-of-the-art simulation resources for the design of photonic ICs.

The unique modeling capabilities developed during this project will have application to several LLNL missions that rely heavily on photonics for secure communication and remote sensing—including advanced laser science, surveillance, stockpile stewardship, and high-bandwidth diagnostics. In addition, high-performance computing, including the ASCI system, can profit from high-density optical interconnects.

During FY01, we focused on modeling basic, all-optical gates realized on both active and passive optical waveguides—specifically, inverter and sampling modules. An inverter (figure (a)) encompasses the proper integration of laser gain elements with dielectric waveguides, with optical inputs and outputs.

We generated suites of 1-D codes using analytical and numerical approaches, in both frequency- and time-domain, to analyze the rate equations for multi-segmented, 1-D lasing devices. We demonstrated both the gain-lever and gain-quenching effects for a two-section, voltage-controlled, Fabry-Perot edge-emitting,

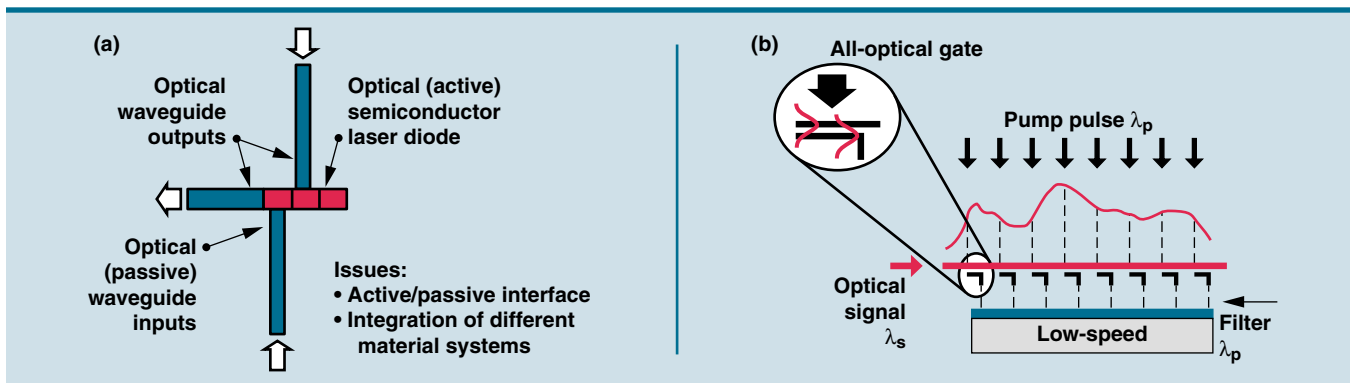
multi-quantum-well laser coupled to a lateral waveguide, injecting light orthogonally to the laser.

Our time-domain codes—which include the longitudinal dependence of the parameters—are written in Java, allowing the development of a flexible GUI. Gain and modulation depth can be obtained using longer control regions and wider lasers, and operating close to threshold. Also, the modulation response improves at the expense of the current, and at higher frequencies (>10 GHz) switching is feasible but level restoring is insufficient.

The sampling modules exploit third-order nonlinearities and are used in a tapped, optical-delay-line architecture (figure (b)) to sample sequential, short-time slices of a transient signal. This allows the use of low-bandwidth detectors to record switched time slices in parallel. We used a beam-propagation method to solve 2-D nonlinear Maxwell equations. Results matched our expectations.

At year’s end, we were examining and optimizing the various parameters, such as length, doping, and mirror reflectivity, affecting the gates in the inverter, and sampling modules in terms of modulation efficiency (level restoring), gain (fan-out), and time response (clock-rate).

In FY02, we plan to include additional physical effects (e.g., spatial hole-burning, wavelength dependencies, and multi-mode structures) and extend the solvers from 1-D to 2-D, and 2-D to 3-D, respectively, for the inverter and sampling gates. We will also continue 1) designing other devices for the final system integration, such as AND, NOR and XOR gates, waveguides, and interfaces; and 2) validating our results against experiment.



Configuration of (a) an all-optical inverter exploiting the gain-quenching effect; and (b) an all-optical tapped delay line, where each sampling gate is a nonlinear directional coupler.

Palm Power: A MEMS-Based Fuel Cell/Integrated Microfluidic Fuel Processor

J. D. Morse, A. F. Jankowski, R. T. Graff, J. P. Hayes

Our miniature fuel cell combines LLNL-developed innovations in materials science and microfabrication capabilities to realize a microfluidic architecture for next-generation power sources. This approach offers a lighter-weight, longer-lasting power source compared to existing rechargeable batteries. Our fuel cell is scalable over a wide range of power levels to meet the requirements of various portable electronics systems.

During FY01 we focused on prototyping fuel cell devices in suitable packages with internal heating elements. Our design included a micromachined support structure fabricated from silicon, in which the anode flow-field structure is designed. A thin film electrode is patterned on the silicon surface in a manner similar to integrated circuit processing. Next a catalyst layer is deposited, followed by a layer of the electrolyte. For the proton exchange membrane fuel cell, the electrolyte is Nafion, a polymer available from Dupont.



Figure 1. Prototype fuel cell package.

The catalyst layers were formed using Pt coatings or inks, which are deposited on the support structure. Electrode meshes were fabricated to provide electrical conduction in a porous structure through which both fuel and air can flow.

An example of a fuel cell package with integrated resistive heaters is shown in Figure 1. The package provides a manifold support for the MEMS-based fuel cell chip, inlet and outlet feeds for the fuel, an air breathing cap, and electrical connections for the heater and power out. Figure 2 is an example of the fuel cell output. The test conditions were: fuel cell temperature, 40 °C; fuel flow, 6.0 sccm of 4% hydrogen in Ar humidified; and air breathing cathode.

Future work will explore specific fuel cell designs to incorporate direct hydrocarbon fuels, either through the use of direct methanol catalyst materials at the anode, or through integration with a fuel reformer to preprocess the hydrocarbon fuel.

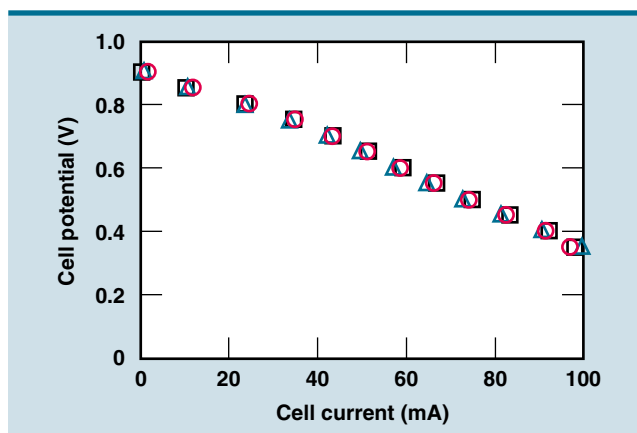


Figure 2. Current-voltage characteristics of MEMS-based fuel cell at 40 °C with 6 sccm of Ar-4% H₂ fuel.

Reconfigurable Optical Code Division Multiple Access (O-CDMA) for Fiber Optical Networks

S. W. Bond, I. Y. Han, S. C. Wilks, E. M. Behymer, V. R. Sperry, S. J. Yoo (University of California, Davis)

By applying innovations in component technology from the wavelength division multiplexing (WDM) market, we are researching a concept for a compact code division multiple access (O-CDMA) encoding and decoding device that would be completely compatible with commercial coding schemes, but that has the enhanced capability of allowing remote, rapidly reconfigurable user codes.

High-speed, high-capacity fiber-optic communications networks—which allow multiple users to access the same network simultaneously by sharing the same transmission medium—have proliferated for long distance, metropolitan, and local area communications systems.

Recently, a rapid expansion into WDM systems, which use multiple wavelengths to increase capacity, is taking place. In addition, it has been recognized that CDMA techniques, which were originally developed for wireless communications, can also be used to further multiplex users on an optical fiber. Fiber networks, which use WDM and CDMA, will be the most important medium for the transfer of information worldwide for the foreseeable future.

We are developing advanced technologies that have potential applications to national security, and that position the Laboratory, in cooperation with government agencies, to better understand and use these systems.

Our approach for a compact O-CDMA encoding and decoding device is to use the techniques of O-CDMA, where each user imprints his own message bits with his own unique code, to spectrally phase modulate (encode) a broadband ultra-short transmitted optical pulse, which can only be decoded by the complementary phase modulation at the receiver end.

The figure shows an example of measured data indicating the effectiveness of a particular code. Our realization is that integrated monolithic semiconductor devices, which do the spectral slicing and phase modulation of the input pulse, can be devised. These will allow for high-speed remote reconfiguration of a user's O-CDMA code.

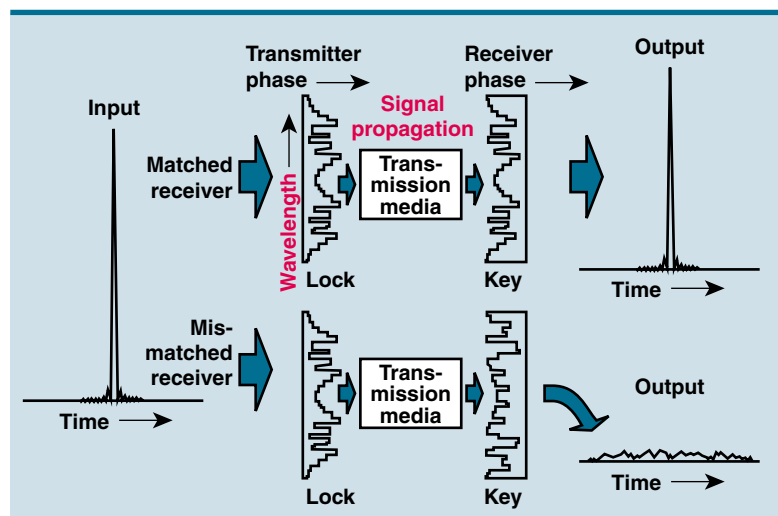
Our approach uses broadband, ultra-fast (300 fs) pulses from a mode-locked Er-doped fiber ring laser operating at $\lambda = 1.55 \mu\text{m}$,

with a 2.5-GHz repetition rate (equivalent to a SONET OC-48 rate). These pulses are spectrally phase-encoded by transmitting them through the monolithically integrated semiconductor device comprised of two arrayed waveguide gratings (AWG) and several phase modulators. The two AWGs do the spectral slicing and recombining of the pulse. Each spectral slice is phase-delayed using an electrically controlled waveguide phase modulator.

This device will allow remote phase trimming of each spectral slice of the input pulse at very high speeds, and forms the basis for long-phase codes that can be reconfigured rapidly.

In FY01 we accomplished the re-initialization of the Metal-Organic Chemical Vapor Deposition (MOCVD) reactor facility at LLNL. We have successfully grown and characterized lattice-matched materials with varying compositions important for the AWG device. Through our collaboration with UC Davis, we have developed several device designs and fabrication methodologies. We have begun modeling the effects of transmission of CDMA-encoded signals across standard fiber-optic networks and are evaluating our ability to compensate for the cumulative propagation effects.

Lastly, we have designed, purchased, and aligned a free space test-bed for the O-CDMA concepts and devices. We are doing initial system alignment and characterization, and expect to demonstrate remote configuration of spectral phase encoded signals in FY02. In FY02 we will fabricate, characterize, and package the integrated semiconductor device.



Example of measured data (with acknowledgment to J. P. Heritage, UC Davis).

Center for Nondestructive Characterization



Technology

Dynamic Focusing of Acoustic Energy for Nondestructive Evaluation

J. V. Candy

The dynamic focusing of acoustic energy is a technique with a large number of applications, ranging from detecting flaws in lenses for laser-based optics to component parts of sensitive weapon systems, each from a nondestructive evaluation (NDE) perspective. In the biomedical area, the focusing of acoustic energy can lead to revolutionary approaches to surgery or mass removal and treatment, as well as enabling efficient delivery of cancer-killing drugs. The ability to focus either acoustic or electromagnetic energy can have a huge impact in developing new methods for secure communications as well as seismic applications in locating underground structures. In any case, the results of this research will lead to a wide variety of applications of high interest to LLNL.

This project is concerned with the research and development of an ultrasonic technique that dynamically focuses acoustic energy to detect and localize flaws for NDE. The impact of this project will be considerable for inspecting optics at the National Ignition Facility and component parts for stockpile stewardship, for noninvasive treatments in the biomedical area, and for secure communications.

We have taken a systematic approach, incorporating detailed simulations, algorithm development, hardware, proof-of-principle NDE experiments and prototype design of a viable flaw detection/localization/imaging system.

Dynamic focusing is achieved by using time-reversal (T/R), a technique to focus on a reflective target or mass through a homogeneous or inhomogeneous medium excited by a broadband source. The T/R processor can be used effectively to detect flaws (or scatterers) by using its primary attribute—the ability to iteratively focus on the strongest flaw.

A T/R processor simply receives the multichannel time series radiated from the region under investigation, collects the array data, digitizes, time-reverses

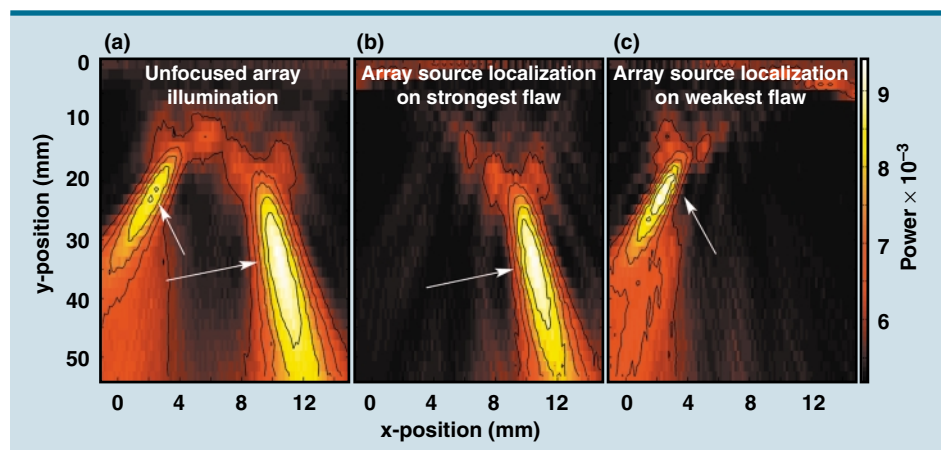
the sensor array signals, and re-transmits them back through the medium to focus.

During this final year, we expanded the scope of the project. We initiated collaborations with researchers at both Stanford and Iowa State Universities, investigating T/R processing techniques for random media and multi-mode scattering structures, respectively.

We are organizing and chairing a topical meeting on T/R in Acoustics under the sponsorship of the Acoustical Society of America. As part of our exit plan, we have developed, conceptually and theoretically, an approach to treat tissue masses using T/R focusing. This is detailed in a proprietary document.

Finally, we completed the development of a prototype T/R instrument for ultrasonic NDE and performed a wide variety of proof-of-principle NDE experiments, such as flaw detection and localization in aluminum (W program) and laser optics (NIF program) as well as a layered composite (ADAPT program).

As one of the experiments, we selectively focused on the strongest flaw in an optic and then on the weaker flaw (see figure), demonstrating the focusing capability using T/R processing. The idea was to compare the iterative focusing capability of the T/R processor to an eigen-decomposition approach using the T/R operator directly in the optic. The results demonstrate that both approaches are capable of focusing ultrasonic energy on the strongest flaw—a very important problem in NIF optics.



Selective dynamic focusing of acoustic energy using T/R prototype system: (a) sixteen-element array with 1-mm spacing at 5 MHz and optic with two flaws; (b) T/R focusing on strongest flaw; (c) T/R focusing on weakest flaw.

High-Accuracy Tomography of Mesoscale Targets

W. Nederbragt, S. Lane, D. Schneberk, T. Barbee, J. L. Klingmann

High-Energy-Density Experiments play an important role in corroborating the improved physics codes that underlie LLNL's Stockpile Stewardship mission. Conducting these experiments, whether on NIF or another national facility such as Omega, will require improvement not only in the diagnostics for measuring the experiment, but also in the fabrication and characterization of the target assemblies.

The characterization of target assemblies is as important as their fabrication because the actual target assembly is the input to the experiment; the characterization of the target assembly is the input to the physics simulation. With this in mind, a radical improvement is needed in characterizing the target assemblies that comprise millimeter-sized components with micrometer-sized features.

X-ray radiography/tomography is one technique that holds promise for characterizing the internal structure of target assemblies. Sub-micrometer spatial resolution has been demonstrated using a synchrotron x-ray source. This approach ill accommodates our requirements for high throughput and low cost for characterizing production quantities of target assemblies.

This project is funding the investigation and development of a Wölter x-ray microscope/tomoscope. If successful, this instrument will provide high-throughput and high-resolution tomography of target assemblies in a laboratory setting. Moreover, this instrument would bring a new capability to the Laboratory that can be used in a variety of areas.

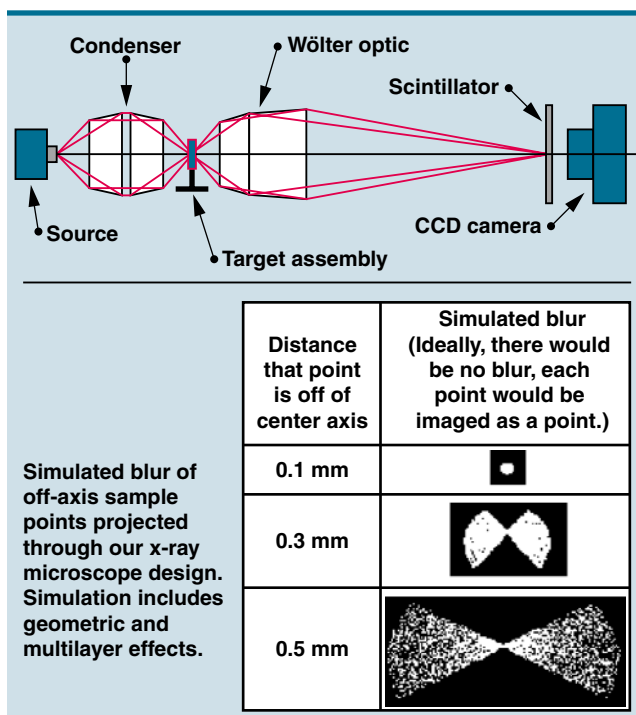
During the last half of FY01, we worked on the preliminary design so that construction could be started in FY02. We began by determining the requirements for the instrument. This included the determination of the x-ray energy needed to penetrate the targets. Based on these calculations and the multilayer coating constraints, we will be using 8-keV photons.

We have also done extensive tests on standard scintillator materials to determine the best material and thickness for our application. Since the scintillator adds to the blur captured by the CCD camera, it is essential to understand the properties of the available choices.

Currently, we are simulating various aspects of the Wölter x-ray instrument. These simulations allow us to vary parameters and find a suitable design that meets our goals. They also allow us to study the effects of the multilayer coatings that will be applied to our optics. These coatings increase the throughput of the instrument and limit the bandwidth of photon energies that are reflected. One problem with the limited bandwidth is that it reduces throughput of off-axis points. The simulations illustrate this effect (see figure).

By the end of FY01, we will have completed our preliminary simulations and will have a preliminary optical design.

In FY02, we will finish the optical design, complete the mechanical design, modify radiography and tomography codes for use with the instrument, and fabricate the optics. In FY03, we will construct the instrument. We will then test and refine the system for use with target assemblies. Ideally, this instrument will lead to the construction of a production instrument for use in the future.



Layout of x-ray microscope/tomoscope.

New Simulation and Reconstruction Algorithms for Quantitative Tomography

M. B. Aufderheide, III, H. E. Martz, Jr., D. M. Goodman, A. Schach von Wittenau, C. M. Logan, J. A. Jackson, D. M. Slone, J. M. Hall

In this project we sought to improve the accuracy of tomographic reconstruction by including the true physics of the radiographic process. The project had two main components. First, we improved our simulation of the radiographic process by improving our modeling of detector and source physics in x-ray radiography, and validating these algorithms against experimental data. Second, we merged this more accurate simulation capability with the Constrained Conjugate Gradient (CCG) optimizer to perform physically accurate forward and back projections required in the tomographic inversion process. This work was expected to improve reconstructions by preventing the mixing of radiographic artifacts with the object reconstruction. After three years of work, we have achieved 2% agreement with data and we have merged the codes and applied this algorithm to several test cases.

Our simulation efforts focused on improving the HADES radiographic simulation code. HADES uses ray-tracing to simulate radiography. The current project improved the code's modeling of detectors and sources. The Monte Carlo transport code, MCNP, was used to determine detector response. This information is then saved in a format that HADES uses in post-processing simulations. Recent application of these techniques to modeling copper step wedges radiographed with LLNL's 9-MeV linac, and using a Varian amorphous silicon flat panel detector, has demonstrated that HADES is accurate at the 2% level. These results will be reported at the IEEE Medical Imaging Conference.

Essentially all tomography algorithms linearize radiography because they assume Beer's law and require logarithms of the experimental images as input. But no experimental data obeys Beer's law, since x-ray sources

are almost never monochromatic. We decided to attack the full nonlinear problem of radiography, since it is faithfully modeled in HADES. Optimizing the full problem has proved challenging. Derivatives of the system become complex, require careful attention to the presence of different materials, and make forward- and back-projection steps complex.

To make this problem tractable, it was necessary to require that the user fix the location of materials within the object. This is a reasonable requirement in many applications. The CCG optimizer had to be modified to treat multiple materials. A simple cone-beam ray-tracing code was connected to the multi-material CCG code to create the MCONE_CCG code. This code was used with simulated data to study the effectiveness of the multi-material algorithm.

At the same time, the HADES and modified CCG codes were operationally linked. HADES required major modifications in its dataflow to compute both forward and back projections over multiple view angles, since it was designed to perform a forward projection at one angle only. In addition to modifying existing forward and back projectors, we decided to have HADES calculate the gradients and search directions required by CCG rather than pass large amounts of redundant data between the two codes. The computational cost of a reconstruction is considerable; the memory cost is also substantial.

We have applied these algorithms to a number of fairly simple problems and will continue refining the techniques in the future. We have found that the algorithm is sensitive to inaccuracies in the data. This sensitivity results from the nonlinearity of the system. We have continued to refine the CCG algorithm for these large problems and have looked at the physics of proton radiography for tomographic reconstruction.

Photothermal Imaging Microscopy

D. Chinn, R. Huber, C. Stolz, P.-K. Kuo (Wayne State University)

Photothermal microscopy (PTM) is a powerful tool for nondestructive evaluation of surface and subsurface structures. By measuring localized optical absorption at discrete laser wavelengths, PTM can map optical absorption, scattering, and reflectivity as well as thermal absorption in materials. PTM has proved very useful in characterizing optical coatings.

In its current state, photothermal scanning microscopy (PTSM) is a raster scanning technique and is limited by extremely slow imaging times. For example, imaging a 1-cm² area of a thin film coating at 10- μ m resolution would take about 278 h. This scan time is too long to make PTSM feasible for coatings on full-sized optics; e.g., NIF mirrors measure approximately 0.4 m \times 0.4 m.

This year we developed photothermal imaging microscopy (PTIM) to make PTM a viable technique for inspecting coatings on full-sized optics. PTIM is a rapid photothermal imaging method that uses focal array detectors and optical lock-in imaging techniques to increase the imaging speed of PTM by a factor of about 10,000.

The test configuration for PTIM is shown in Figure 1. The pump beam illuminates a \sim 5-mm-diameter area of the test surface. Surface and subsurface defects within the test area absorb the light and cause a surface “bump” to form, from thermal deformation. The surface deformation diffracts the probe laser. The resultant field is recorded by a 1024- \times -1024-pixel CCD camera. Chopping the pump beam and locking in the probe beam to the chopping frequency improves sensitivity to the photothermal response. By applying optical lock-in techniques to the camera images, we obtain a PTIM image.

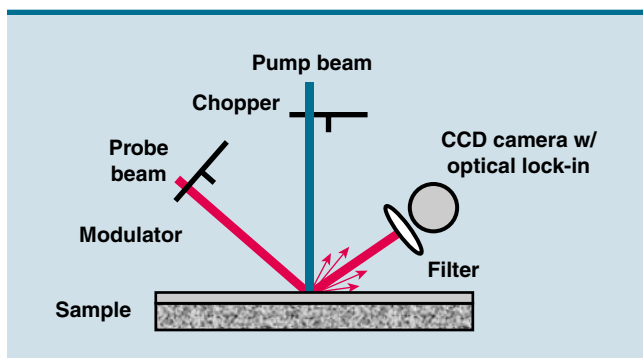


Figure 1. PTIM schematic, showing collimated pump beam (5 mm dia., $\lambda = 532$ nm) and probe beam (5 mm dia., $\lambda = 633$ nm).

Figure 2 shows a PTIM image of a BK7 glass sample with an anti-reflective coating. Aluminum dots are sputtered onto the glass substrate before coating. PTIM gives comparable images to PTSM of the aluminum absorber. For the small area around the aluminum dot, imaging time is decreased by a factor of 50.

Figure 3 shows normalized PTSM, PTIM and theoretical amplitude profiles of the photothermal response across the aluminum dot. The diffraction theory curve assumes a Gaussian probe beam and a Gaussian-shaped “bump” resulting from heating of the aluminum dot. Both PTSM and PTIM profiles correlate well with the modeled profile.

By proving the principle of PTIM, we developed a capability that does not exist anywhere else in the world. This multi-programmatic capability will help NIF coating engineers determine the source and characteristics of defects, help microtechnology engineers assess lithography techniques, and possibly help EUV lithography engineers find defects in multilayer structures. The technology will reduce inspection time by 5.5 orders of magnitude; i.e., inspection of a 5-mm- \times -5-mm area of NIF optical coating at 5 μ m resolution will decrease from 278 h to 2 s.

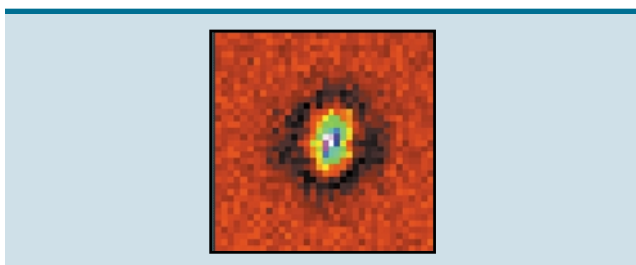


Figure 2. PTIM image of a sputtered aluminum dot.

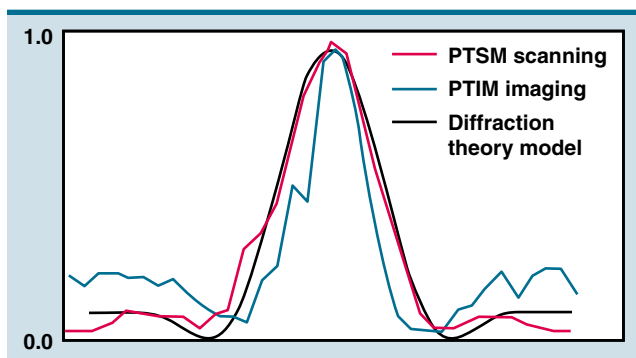


Figure 3. Normalized amplitude profile across the aluminum dot.

Center for Precision Engineering



Technology

Predicting Precise Deformation of Non-Rigid Objects

K. L. Blaedel, D. W. Swift, A. A. Claudet

Dimensional characterization of non-rigid parts presents many challenges. For example, when a non-rigid part is mounted in an inspection apparatus, the effect of the fixturing is significant. If the part is not used in normal service with the same load conditions as during inspection, the dimensional characteristics will certainly deviate from reported values. Further, the solution of designing specialized fixturing to duplicate "as-installed" conditions does not resolve the problem. For rigid objects, measurement standards are generally of a known pedigree that can be traced to a central authority (e.g., NIST). There is no analog of that tractability to a single source for non-rigid parts. Specialized fixturing for specific cases precludes standardization across different parts and different manufacturers.

The non-rigid metrology problem is of direct interest to LLNL in at least three ways. First, it has implications concerning the characterization of thin, hemispherical shells. Second, it has application to the metrology of thin photomasks for extreme-ultraviolet lithography (EUVL). Third, it can help in the inspection of potassium dihydrogen phosphate (KDP) crystals in advanced laser systems. It is important to industry because it has applications to metrology of sheet-metal parts.

The goal of this project is to formulate the research problem and propose a method of assessing the dimensional characteristics of non-rigid parts. The central idea is the concept of a "free shape." The free shape is the geometry of the part when no loads are present, i.e., when those loads produced by fixturing, gravity, and others are not present. Since it is impossible to directly measure the free shape, some method for inferring it must be developed. Once the free shape is

known, some metric must be developed for acceptance or rejection of the part.

In FY01 a copper test cylinder and fixturing apparatus were developed (see figures). The cylinder was carefully manufactured under conditions designed to facilitate later analysis. The fixturing apparatus applies known loads at three points equally distributed around the cylinder. When the cylinder is in the fixture, the only loads acting on it are those from the three actuators and gravity. Several load conditions were prescribed and 3-D measurements of the cylinder were taken. The loads were computed so that there were five equal steps that deformed the cylinder approximately 2% of its thickness.

The combination of the known load conditions and the geometric configuration induced by those conditions allows a finite element analysis to be performed. The goal of the finite element analysis is to find the relation between the loads and geometry so that the geometry at a zero load condition, the free shape, can be extrapolated.

With the free shape geometry known, an energy metric is computed to determine the quality of the part. For each node of the finite element model, a corresponding closest-point projection is made onto the ideal geometry. The finite element nodes are then forced onto the ideal geometry and reaction forces computed. The metric is the sum of the reaction forces for each node multiplied by the deviation of the node in the free shape from its projection onto the ideal geometry.

The knowledge gained from this project provides a better understanding of non-rigid metrology. Future publications will make the problem a more salient research issue.

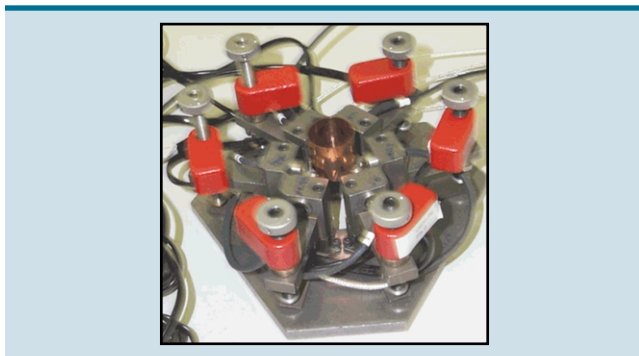


Figure 1. Known fixturing condition.

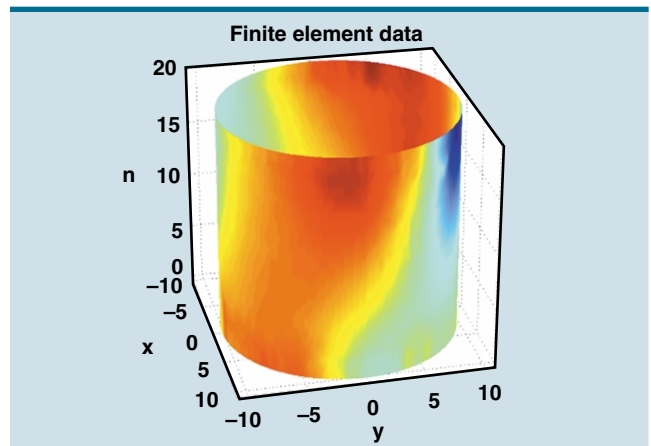


Figure 2. Free shape.

Author Index

Technology

Author Index

Aufderheide, III, M. B.	29	Logan, C. M.	29
Barbee, T.	28	Martz, Jr., H. E.	29
Becker, R.	12	McCallen, D. B.	4
Behymer, E. M.	23	McMahon, D. H.	4
Benett, W.	17, 18, 19	Miles, R. R.	19
Bentley, L.	19	Mish, K. D.	14
Blaedel, K. L.	33	Morse, J. D.	20, 22
Bond, S. W.	23	Nederbragt, W.	28
Bond, T. C.	21	Ness, K.	18
Candy, J. V.	27	Paglieroni, D. W.	5
Champagne, II, N. J.	10, 13	Papavasiliou, A.	18
Chinn, D.	30	Perkins, D. E.	5
Clague, D. S.	11	Pocha, M. D.	21
Claudet, A. A.	33	Puso, M. A.	9
Dowla, F. U.	6	Richards, J.	18
Fisher, K.	17	Roberts, R.	3
Ford, G. E.	5	Rock, D. W.	4
Goodman, D. M.	29	Schach von Wittenau, A.	29
Graff, R. T.	20, 22	Schneberk, D.	28
Hall, J. M.	29	Seward, K.	19
Han, I. Y.	23	Sharpe, R. M.	10, 13
Harris, D. B.	4	Slone, D. M.	29
Hayes, J. P.	20, 22	Sperry, V. R.	23
Huber, R.	30	Stephan, P.	19
Jackson, J. A.	29	Stolz, C.	30
Jankowski, A. F.	20, 22	Stratton, P.	18
Kellman, J. K.	21	Swift, D. W.	33
Khanaka, G. H.	21	Tarte, L.	17
Klingmann, J. L.	28	Tendick, F.	19
Kuo, P.-K.	30	Wang, A.	17
Lane, S.	28	Weisgraber, T.	18
Larsen, S. C.	4	Wheeler, E. K.	11, 18
Lee, C.	17	White, D. A.	10, 13
Levatin, J. L.	4	Wilks, S. C.	23
Lewis, J. P.	4	Yoo, S. J.	23

Manuscript Date September 2002
Distribution Category UC-42

This report has been reproduced directly from the best available copy.

Available for a processing fee to U.S. Department of Energy
and its contractors in paper from
U.S. Department of Energy
Office of Scientific and Technical Information
P.O. Box 62
Oak Ridge, TN 37831-0062
Telephone: (865) 576-8401
Facsimile: (865) 576-5728
E-mail: reports@adonis.osti.gov
Available for sale to the public from
U.S. Department of Commerce
National Technical Information Service
5285 Port Royal Road
Springfield, VA 22161
Telephone: (800) 553-6847
Facsimile: (703) 605-6900
E-mail: orders@ntis.fedworld.gov
Online ordering: <http://www.ntis.gov/ordering.htm>
OR

Lawrence Livermore National Laboratory
Technical Information Department's Digital Library
<http://www.llnl.gov/tid/Library.html>

This document was prepared as an account of work sponsored by an agency of the United States Government. Neither the United States Government nor the University of California nor any of their employees, makes any warranty, express or implied, or assumes any legal liability or responsibility for the accuracy, completeness, or usefulness of any information, apparatus, product, or process disclosed, or represents that its use would not infringe privately owned rights. Reference herein to any specific commercial products, process, or service by trade name, trademark, manufacturer, or otherwise, does not necessarily constitute or imply its endorsement, recommendation, or favoring by the United States Government or the University of California. The views and opinions of authors expressed herein do not necessarily state or reflect those of the United States Government or the University of California, and shall not be used for advertising or product endorsement purposes.

Work performed under the auspices of the U.S. Department of Energy by the University of California, Lawrence Livermore National Laboratory under Contract W-7405-Eng-48.
ENG-01-0043a-AD



Engineering Directorate
Lawrence Livermore National Laboratory
University of California
P.O. Box 808, L-124
Livermore, California 94551

<http://www-eng.llnl.gov/>

Engineering